ISSN 1070-3632, Russian Journal of General Chemistry, 2008, Vol. 78, No. 3, pp. 376–382. © Pleiades Publishing, Ltd., 2008.
Original Russian Text © N.A. Zhuk, I.V. Piir, N.V. Chezhina, 2008, published in Zhurnal Obshchei Khimii, 2008, Vol. 78, No. 3, pp. 393–399.

Structure, Magnetic, and Electric Properties of Bismuth Niobates Doped with *d*-Elements: VI.[1] Magnetic Behavior of $Bi_3Nb_{3-3x}Ni_{3x}O_{15-\delta}$ Solid Solutions

N. A. Zhuk[a], I. V. Piir[a], and N. V. Chezhina[b]

[a] *Syktyvkar State University, Syktyvkar, Russia*
[b] *St. Petersburg State University, Universitetskii pr. 26, St. Petersburg, 198504 Russia*

Received July 5, 2007

Abstract—Magnetic susceptibility of nickel-containing solid solutions with layered perovskite-like structure of bismuth niobate, $Bi_5Nb_3O_{15}$, was studied. High-spin nickel atoms, Ni(III), were present at low concentrations of the solid solutions. The formation of exchange-bonded aggregates (dimers) of nickel(II) atoms with antiferromagnetic type of exchange was found in the solid solutions. The parameters of exchange interactions in the dimer clusters and the distribution of monomers and dimers of nickel atoms were calculated as a function of the solid solution concentration.

DOI: 10.1134/S1070363208030079

Former studies of magnetic dilution in the solid solutions of bismuth orthoniobate $BiNb_{1-x}M_xO_{4-\delta}$ and bismuth niobate of $Bi_3Nb_{3-3x}M_{3x}O_{15-\delta}$ (M is Cr, Ni, Cu) [1–3] suggest that the substitution of atoms with a lower valence (chromium, copper, and nickel) for niobium is accompanied by a partial oxidation of paramagnetic atoms at a low concentration. This ensures a compensation of the charge misbalance resulting from the heterovalent substitution. This work describes the magnetochemical study of the state of nickel atoms and of exchange interactions in the solid solutions in bismuth niobate $Bi_5Nb_3O_{15}$ obtained by heterovalent substitution of nickel atoms for niobium.

Bismuth niobate, $Bi_5Nb_3O_{15}$, belongs to mixed layered perovskite-like compounds with a crystal structure characterized by an ordered alternation of niobium-oxygen layers one and two octahedra thick. Large bismuth cations are located in the cubic octahedral voids formed by the layers of two octahedra in thickness. The layers of niobium-oxygen octahedra are separated by bismuth-oxygen layers formed by BiO_4 pyramids and bound to each other by the edges of the bases. The crystal structure of bismuth niobate can be described assuming the space group to be *P*4/*mmm* with the unit cell parameters *a* 0.547and *c* 2.097 nm [4].

The $Bi_3Nb_{3-3x}Ni_{3x}O_{15-\delta}$ solid solutions were prepared with $x < 0.08$. We found that the tetragonal cell undergoes a monoclinic distortion as the concentration of the solid solutions increased ($x \geq 0.02$). The X-ray pattern of the solid solutions with $x < 0.02$ were indexed assuming the space group to be *P*4/*mmm*, and that of the solid solutions with $x \geq 0.02$, *P*2/*m* [4]. We calculated the unit cell parameters by the least-squares method (Table 1). We found that the parameters *a* and *c* moderately increase and the angle α changes from 90° to 91.11° as the concentration of the solid solution grows.

On the basis of measured magnetic susceptibility of the solid solutions we calculated paramagnetic components of magnetic susceptibility [χ^{para}(Ni)] and effective magnetic moments [μ_{eff}(Ni)] of nickel atoms at various temperatures and for various concentrations of nickel in the solid solutions. We introduced diamagnetic corrections to the calculated paramagnetic component of magnetic susceptibility with regard to the susceptibility of $Bi_5Nb_3O_{15}$ matrix measured over the same temperature range. The dependence of the inverse molar paramagnetic component of magnetic susceptibility of nickel atoms on temperature obeys Curie–Weiss law in the temperature range under study for all the solid solutions. The paramagnetic component of nickel magnetic susceptibility decreases as

[1] For communication V, see [1].

Table 1. Interatomic distances and angles in the unit cell of $Bi_3Nb_{3-3x}Ni_{3x}O_{15-\delta}$

Parameter	$Bi_5Nb_{3-3x}Ni_{3x}O_{15-\delta}$, $Bi_5Nb_3O_{15}$	*x* 0.005	*x* 0.01	*x* 0.02	*x* 0.03	*x* 0.04	*x* 0.06	*x* 0.08
a, Å	5.472	5.471	5.472	5.474	5.476	5.480	5.482	5.487
b, Å	5.472			5.469	5.466	5.459	5.458	5.455
c, Å	20.97	20.96	20.98	20.98	21.00	21.05	21.02	21.03
α, deg	90			89.92	90.41	90.57	90.70	91.11

the concentration of the solid solution increases, which is typical for the dilution of antiferromagnetics (Fig. 1). The extrapolation of the isotherms of paramagnetic component of magnetic susceptibility to zero concentration of the solid solution led to the calculation of the temperature dependencies of χ^{para}(Ni) and of effective magnetic moment for a lone paramagnetic atom. The effective magnetic moments of nickel atoms in the $Bi_3Nb_{3-3x}Ni_{3x}O_{15-\delta}$ compound at $x \to 0$ are given below. The effective magnetic moment of nickel atoms depends on temperature. Its values are between the spin only values for low-spin nickel, Ni(III), [μ_{eff}(Ni (III) 1.73 BM], nickel(II) [μ_{eff}(Ni(II) 2.88 BM] and high-spin nickel, Ni(III), [μ_{eff}(Ni(III) 3.87 BM]. The temperature dependence of the effective magnetic moments of nickel atoms extrapolated to infinite dilution points to the presence of nickel(III) atoms in the high-spin state with the ground term $^4T_{1g}$ (S 3/2).

T, K	77	90	100	120	160	180	220	300
μ, BM	3.43	3.49	3.52	3.59	3.67	3.69	3.75	3.80

In the ESR spectra of the solid solutions under study (*x* 0.005) a wide anisotropic line is observed with *g* 2.35 indicating the presence of Ni(II) atoms, but no signal from low spin nickel(III) was found.

Hence we concluded that at $x \to 0$ nickel(II) and high-spin nickel(III) atoms were present in the solid solutions.

Since the magnetic moment of paramagnetic nickel atoms is the sum of the contributions of the magnetic moments of the available Ni(II) and Ni(III) atoms, we can estimate the fractions of corresponding nickel atoms in the solid solutions by formula (1).

$$\mu^2_{exp} = b\mu^2_{Ni(II)} + (1 - b)\mu^2_{Ni(III)}. \quad (1)$$

Here μ_{exp} is the experimental magnetic moments found by the extrapolation of the isotherms of magnetic susceptibility, χ^{para}(Ni), to the infinite dilution followed by calculation of μ_{exp}, *b* is the fraction of nickel atoms, Ni(II), $\mu_{Ni(II)}$ is the spin only value of magnetic moment of nickel(II), and $\mu_{Ni(III)}$ is the magnetic moment of high-spin nickel(III) atoms. Note that the magnetic moment of high-spin nickel(III) atoms having a triply degenerated ground term (term $^4T_{1g}$) depends on temperature. Hence we carried out an additional calculation of magnetic moment, $\mu_{Ni(III)}$, for each temperature by formula (2) [5]. The calculated data are given in Table 2.

$$\mu^2_{Ni(III)} = \frac{3[3.15x + 3.92 + (2.84x + 2.13)e^{(-15x/4) + (4.7x - 6.05)}e^{(-6x)}]}{x[3 + 2e^{(-15x/4)} + e^{(-6x)}]}. \quad (2)$$

Here $x = \lambda_2/kT$, λ_2 is the spin-orbital coupling constant, its estimation is given in [3], *k* is the Boltzmann constant, and *T* is the absolute temperature.

The calculated fraction of nickel(III) atoms is ~30%. A decrease in the magnetic susceptibility of nickel with increasing concentration of the solid solution and an increase in the magnetic moment with increasing temperature point to antiferromagnetic exchange interactions between nickel atoms (Fig. 2). The superexchange interactions can take place in the

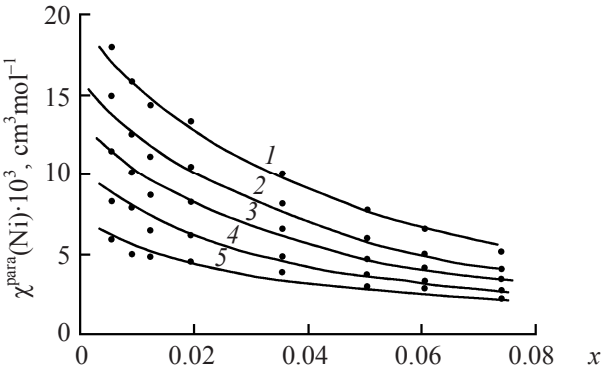

Fig. 1. Isotherms of the paramagnetic component of magnetic susceptibility of the $Bi_3Nb_{3-3x}Ni_{3x}O_{15-\delta}$ solid solutions at *T*: (*1*) 90, (*2*) 120, (*3*) 160, (*4*) 220, (*5*) 300 K.

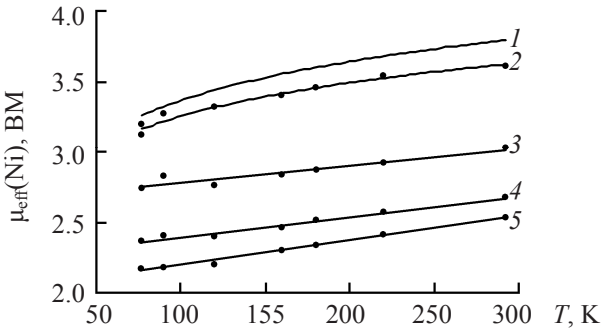

Fig. 2. Plot of magnetic moment of nickel atoms, μ_{eff}(Ni), vs. temperature at x: (*1*) 0.009, (*2*) 0.025, (*3*) 0.036, (*4*) 0.050, (*5*) 0.061.

dimers between Ni(II)–O–Ni(II) atoms, between high-spin nickel atoms, Ni(III)–O–Ni(III), and in the mixed Ni(III)–O–Ni(II) dimers predominantly by the $d_{x^2-y^2}||p_x||d_{x^2-y^2}$, $d_z2||p_z||d_{z^2}$, $d_{xy}|p_y|d_{xy}$ channels of orbital overlapping. Since in the infinitely diluted solid solution the fraction of nickel(III) atoms is small that eventually affects the number of dimers formed by them, we calculated the magnetic susceptibility assuming that dimers are formed only by Ni(II) atoms (3).

$$\chi^{para}_{calc}(Ni) = a^{mon}_{Ni(III)}\chi^{mon}_{Ni(III)} + (1 - a^{mon}_{Ni(III)}) \times [a^{mon}_{Ni(II)}\chi^{mon}_{Ni(II)} + (1 - a^{mon}_{Ni(II)}\chi^{dim}_{Ni(II)-Ni(II)}]. \quad (3)$$

Here $\chi^{mon}_{Ni(II)}$ and $\chi^{mon}_{Ni(III)}$ are magnetic susceptibilities of nickel(II) and high-spin nickel(III) atoms, respectively; $\chi^{dim}_{Ni(II)-Ni(II)}$ is magnetic susceptibility of the Ni(II)–O–Ni(II) dimers, $a^{mon}_{Ni(II)}$ and $a^{mon}_{Ni(III)}$ are fractions of Ni(II) and Ni(III) monomers. The fraction of the dimers is given as a fraction of the total fraction of nickel(II) atoms (Table 3). Formula (3) contains three independent parameters: the fractions of isolated Ni(III) and Ni(II) atoms (monomers), and the parameter of antiferromagnetic exchange between nickel(II) atoms implicitly included into the formula, $J_{Ni(II)-Ni(II)}$.

Table 2. Calculated fractions of nickel(III) atoms, $a_{Ni(III)}$, at $x\to0$

T, K	90	120	160	220	300
λ/kT	–2.72	–2.04	–1.53	–1.11	–0.82
$\mu_{Ni(III)}$, BM	4.55	4.75	4.95	5.12	5.21
$a_{Ni(III)}$	0.335	0.335	0.331	0.333	0.336

The calculation of exchange interactions is based on Heizenberg–Dirack–van Vleck model of isotropic exchange (HDVV) developed for complex compounds containing metal atom clusters. This model gives a mathematic instrument for the description of magnetic properties of any cluster [6]. The paramagnetic component of magnetic susceptibility of a dimer can be estimated by formula (4), and g-factor, by formula (5).

$$\chi_{dim} = \frac{1}{2}\frac{\sum_g g^2(S)S(S+1)(2S+1)e^{-E(J,S)/kT}}{8T\sum_S(2S+1)e^{-E(J,S)/kT}}, \quad (4)$$

$$E(J,S) = -J[S(S+1) - S_a(S_a+1) - S_b(S_b+1),$$

$$S = S_a + S_b, \quad S_a + S_b - 1, \ldots, |S_a - S_b|.$$

$$g(S) = \frac{g_a + g_b}{2} + \frac{g_a - g_b}{2}\frac{S_a(S_a+1) - S_b(S_b+1)}{S(S+1)}. \quad (5)$$

Here S_a and S_b are spins of the atoms making up a dimer [$S_{Ni(II)} = 1$]; g_a and g_b are g-factors for Ni(II) atoms ($g_a = g_b = 2$), J is the exchange parameter, and T is the absolute temperature.

An agreement between calculated and experimental data is achieved by minimization of function (6), possible when a sufficiently large set of concentrations and temperature dependencies of magnetic characteristics is available.

$$\sum_i\sum_j(\chi^{calc}_{ij} - \chi^{exp}_{ij}). \quad (6)$$

Here $\sum_i$ is summing over all concentrations, $\sum_i$ is summing over all temperatures; χ^{exp}_{ij} and χ^{calc}_{ij} are the experimental and calculated paramagnetic components of magnetic susceptibility.

As a result of our calculations we obtained the data on the distribution of nickel atoms in the solid solutions (Table 3). The antiferromagnetic exchange parameter in dimers, $J_{Ni(II)-Ni(II)}$, is –25 cm^{-1}.

The calculation showed the following special features of nickel atom behavior in the solid solutions (Fig. 3). The heterovalent substitution of nickel atoms for niobium atoms in the solid solutions results only in a partial oxidation of Ni(II) atoms to Ni(III). Nickel atoms at infinite dilution are in two valence states, in the form of Ni(II) and high-spin Ni(III) atoms, the fraction of the latter decreases to zero as the concentration of the solid solutions increases. In

Table 3. Calculated distribution of nickel atoms in the $Bi_3Nb_{3-3x}Ni_{3x}O_{15-\delta}$ solid solutions[a]

x	$a^{mon}_{Ni(II)}$	$a_{Ni(II)}$	$a^{dim}_{Ni(II)-Ni(II)}$	$\chi_{exp(theor)} \times 10^6$, cm^3 mol^{-1}				
				90 K	120 K	160 K	220 K	300 K
0.01	0.25	0.75	0.15	14800(14753)	11900(11657)	9400(9184)	6800(6963)	5200(5222)
0.02	0.18	0.82	0.28	12800(12862)	10200(10209)	8400(8062)	6200(6124)	4600(4604)
0.03	0.12	0.88	0.43	11000(10965)	8700(8805)	7100(7007)	5400(5354)	4000(4048)
0.04	0.05	0.95	0.47	9200(9354)	7400(7521)	6000(5979)	4500(4565)	3500(3456)
0.05	0.00	1.00	0.62	7800(7492)	6200(6186)	4800(5005)	3800(3873)	3000(2965)
0.06	0.00	1.00	0.90	6600(5900)	5000(5247)	4200(4466)	3200(3586)	2800(2811)

[a] $a^{mon}_{Ni(III)}$ is the fraction of nickel(III) monomers, $a_{Ni(II)}$ is the fraction of Ni(II) dimers and monomers, $a^{dim}_{Ni(II)-Ni(II)}$ is the fraction of Ni(II)–O–Ni(II) of the $a_{Ni(II)}$ fraction.

perovskites and perovskite-like structures the isovalent substitution usually stabilizes nickel in the trivalent state [5, 7, 8]. In our case it is oxidized only partially, which inevitably results in a greater electron misbalance and should increase the number of vacancies in the oxygen sublattice. However in this case we must suggest that the stability of the structure is provided by the formation of Ni(II) dimers spatially bound to vacancies. A very large fraction of such dimers (0.62 at x 0.05) exceeding by a factor of more than three the statistically probable value (Table 4) supports this suggestion.

It is believed that the compensation of the charge misbalance inevitably resulting from heterovalent substitution is achieved at low concentrations by a partial (or complete) oxidation of introduced paramagnetic atoms. In the case of essentially greater substitution degrees and a greater concentration of the solid solution the compensation mechanism may be different, namely: by the formation of exchange-bound aggregates with oxygen vacancies coordinated in their vicinity, which can favor the crystal lattice stabilization.

We measured the capacitance and the tangent of dielectric losses for the $Bi_3Nb_{3-3x}Ni_{3x}O_{15-\delta}$ solid solutions (x 0.04 and 0.06) and calculated on this basis the dielectric constants and specific conductivities.

The dielectric constant (ε) of the solid solutions moderately changes in the temperature range 300–650 K. Its values are proportional to the frequency of applied field at these temperatures. At $T > 650$ K an increase in the dielectric constant is observed, the more intensive the lower is the frequency of the applied field (Fig. 4). At the frequencies of 100 and 200 kHz the dielectric constant remains almost unchanged. The temperature at which an increase in ε is observed decreases as the concentration of the solid solutions grows. At the background of the overall increase in the dielectric constant its jump is observed at 700 K (x 0.04) found for all the solid solutions. The value of the jump depends on the frequency of the applied field. The temperature at which the jump in ε occurs decreases as the concentration of the solid solution grows, being independent of the field frequency. It can be associated with a ferrielectric ordering.

Two parts may be distinguished on the temperature dependencies of the specific conductivity. Up to a certain temperature depending on the field frequency (x 0.04, T 600 K, ω 1 kHz) the conductivity remains almost unchanged, whereas at higher temperatures it increases obeying Arrhenius equation with the activation energy E_a of 0.16 eV. The temperature of

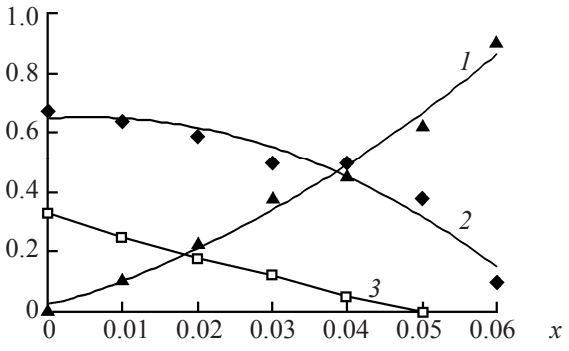

Fig. 3. Plots of the fraction of: (*1*) Ni(II)–O–Ni(II) dimers,(*2*) Ni(II) monomers, and (*3*) Ni(III) monomers vs. con-centration of $Bi_3Nb_{3-3x}Ni_{3x}O_{15-\delta}$ solid solutions.

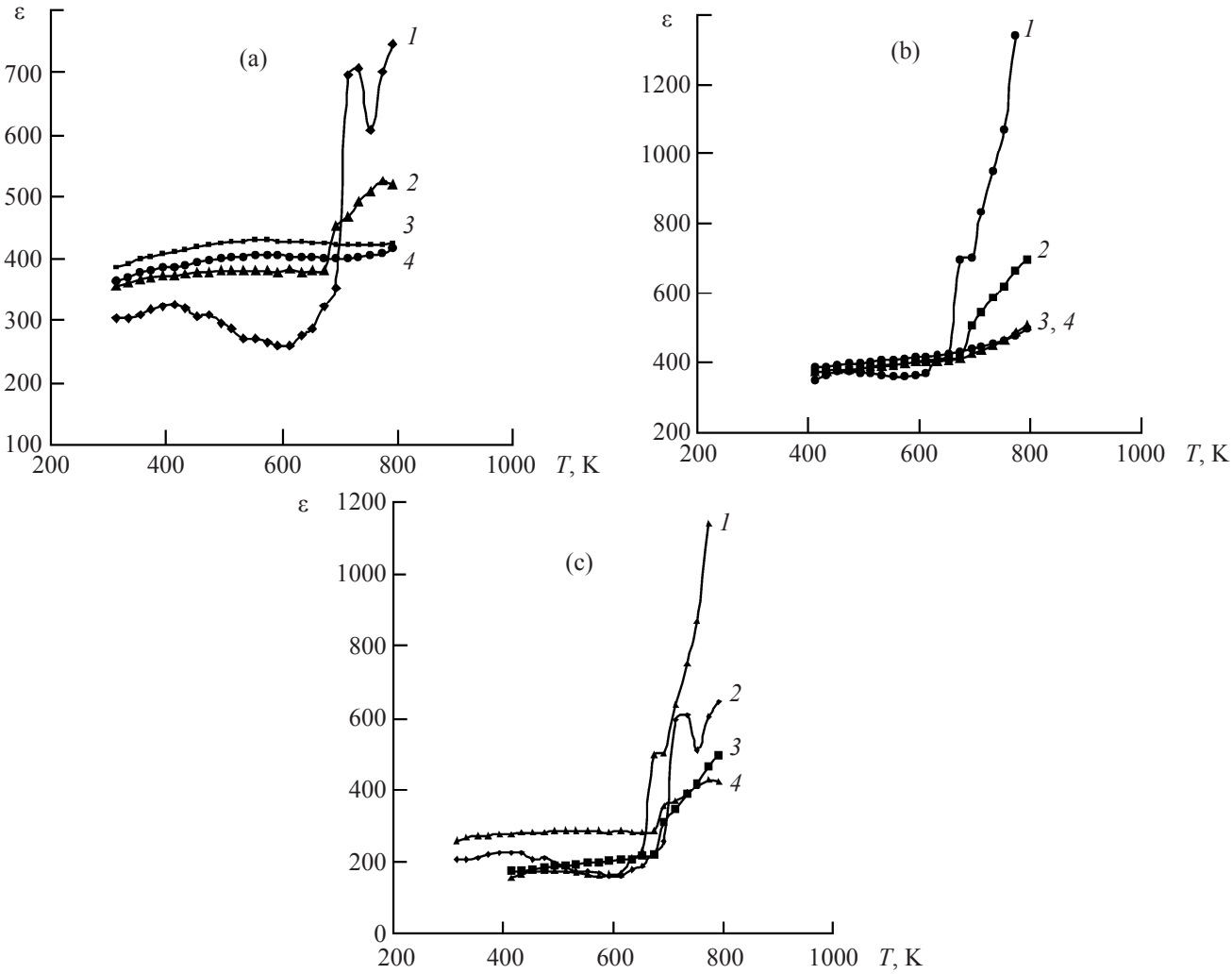

Fig. 4. Temperature dependence of dielectric constant of the $Bi_3Nb_{3-3x}Ni_{3x}O_{15-\delta}$ solid solutions [x: (a) 0.04, (b) 0.06] at the field frequency ω of: (*1*) 1, (*2*) 10, (*3*) 100, (*4*) 200 kHz; (c) x: (*2*), (*4*) 0.04 and (*3*, *6*) 0.06 at the field frequency ω of: (*1, 2*) 1 and (*3, 4*) 10 kHz.

Table 4. Calculated distribution of nickel atoms in the $Bi_3Nb_{3-3x}Ni_{3x}O_{15-\delta}$ solid solutions[a]

x	a_{stat}^{dim}	$a_{Ni(II)–Ni(II)}^{dim}$	$a_{Ni(II)}^{mon}$	$a_{Ni(III)}^{mon}$
0.00	0.00	0.00	0.67	0.33
0.01	0.04	0.11	0.64	0.25
0.02	0.08	0.23	0.59	0.18
0.03	0.11	0.38	0.50	0.12
0.04	0.15	0.45	0.50	0.05
0.05	0.19	0.62	0.38	0.00
0.06	0.22	0.90	0.10	0.00

[a] $a_{N(III)}^{mon}$ and $a_{N(II)}^{mon}$ are fractions of nickel(III) and Ni(II) monomers, $a_{Ni(II)–Ni(II)}^{dim}$ is a fraction of Ni(II)–O–Ni(II) dimers, a_{stat}^{dim} is a statistic fraction of the dimers.

abrupt increase in the specific conductivity is shifted to the region of higher values as the field frequency increases (Figs. 5 and 6). The dependence of specific conductivity on the field frequency points to a mixed electron-ionic type of conductivity. At the temperature corresponding to the ferrielectric transition a jump in the specific conductivity is observed, its value being proportional to the field frequency. As the concentration of the solid solutions grows, the specific conductivity noticeably increases at the field frequency 100–200 kHz. An increase in the dielectric constant and specific conductivity at $T > 600$ K may be associated with ion polarization and the following activation of the ionic-oxygen transfer.

EXPERIMENTAL

The solid solutions were synthesized by prolonged

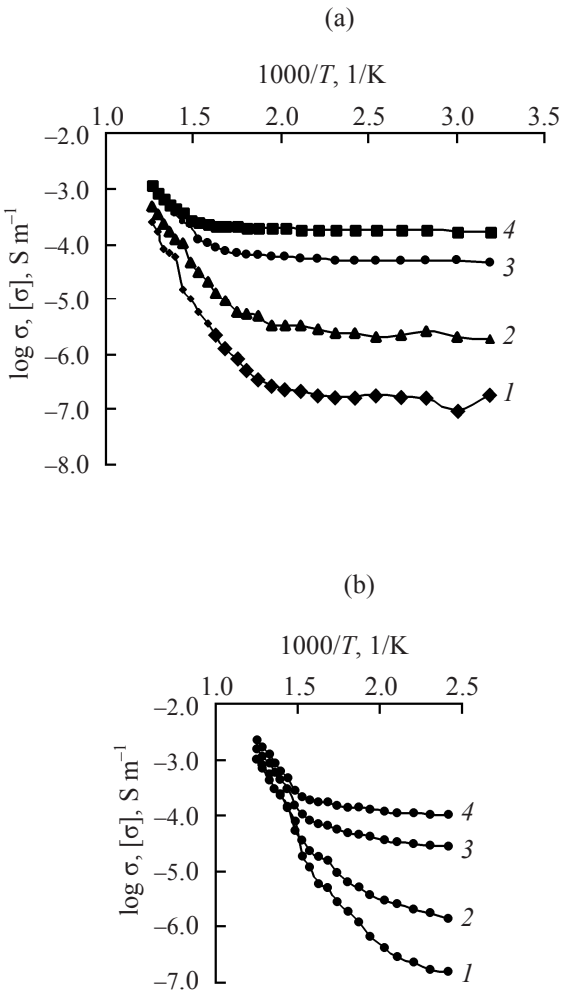

Fig. 5. Temperature dependence of the specific conductivity of the $Bi_3Nb_{3-3x}Ni_{3x}O_{15-\delta}$ solid solutions [*x*: (a) 0.04, (b) 0.06] at the field frequency ω of: (*1*) 1, (*2*) 10, (*3*) 100, (*4*) 200 kHz.

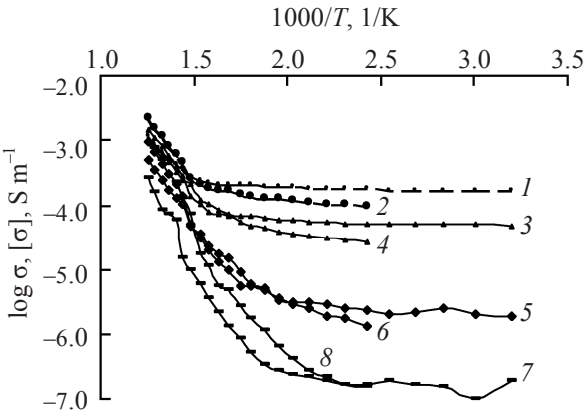

Fig. 6. Temperature dependence of the specific conductivity of the $Bi_3Nb_{3-3x}Ni_{3x}O_{15-\delta}$ solid solutions [*x*: (*1, 3, 5, 7*) 0.0 4 and (*2, 4, 6, 8*) 0.06] at the field frequency ω of: (*7, 8*) 1, (*5, 6*) 10, (*3*, *4*) 100, (*1*, *2*) 200 kHz.

sintering a stoichiometric mixture of especially pure bismuth, niobium, and nickel oxides in the temperature range 650–950°C. We controlled the phase composition of the solid solutions by X-ray analysis (DRON-4-13, CuK_α) and electron scanning microscopy (a JSM 6400 electron microscope). The unit cell parameters of the solid solutions were calculated using the CSD program package [9]. The quantitative analysis of nickel content in the obtained samples was performed by the photometric method. The accuracy of the analysis was ~5% of *x* in the solid solution formula.

The magnetic susceptibility of the solid solutions was measured by Faraday method in the temperature range 77–400 K, the accuracy of the measurements was 2%.

With the aim of studying the state of paramagnetic nickel atoms in the solid solutions we recorded the ESR spectra. The ESR spectra were recorded on an RE 1306 radiospectrometer using a standard modulation procedure. The operation frequency of a resonator was 9.45 GHz. We observed the signals of resonance absorption of paramagnetic atoms at the following parameters: the average field intensity 3300 G and the scan of magnetic field 2000 G. The EPR spectra were recorded at room temperature in thin-walled quarts tubes.

To measure the electrophysical characteristics, a silver current-conducting layer was deposited on the end surfaces of the disk samples. The tangent of dielectric losses and the capacitance of the samples were measured by the two-contact method using an RLC-MT 4090 automatic alternating-current bridge at the field frequencies of 1, 10, 100, and 200 kHz in the temperature range 300–750 K in the heating and cooling mode. The temperature in the operating volume was monitored with a Chromel–Alumel thermocouple.

REFERENCES

1. Zhuk, N.A., Piir, I.V., Pimenov, A.L., and Chezhina, N.V., *Zh. Obshch. Khim*., 2008, vol. 78, no. 3, p. 353.
2. Zhuk, N.A., Piir, I.V., and Chezhina, N.V., *Zh. Obshch. Khim*., 2006, vol. 76, no. 11, p. 1780.
3. Zhuk, N.A., Piir, I.V., and Chezhina, N.V., *Zh. Obshch. Khim*., 2006, vol. 76, no. 11, p. 1786.
4. Yanovskii, V.K., Voronkova, V.I., and Vodolazskaya, I.V., *Neorg. Mater*., 1990, vol. 26, no. 6, p. 1297.

5. Chezhina, N.V. and Kuznetsova, I.V., *Zh. Obshch. Khim*., 1995, vol. 65, no. 5, p. 1068.
6. Kalinnikov, V.T. and Rakitin, Yu.V., *Vvedenie v magnetokhimiyu. Metod staticheskoi magnitnoi vospriimchivosti v khimii* (Introduction to Magnetochemistry. Method of Static Magnetic Susceptibility in Chemistry), Moscow: Nauka, 1980.
7 Chezhina, N.V., *Zh. Obshch. Khim*., 1996, no. 6, p. 911.
8. Chezhina, N.V. and Kuznetsova, I.V., *Zh. Obshch. Khim*., 1999, vol. 69, no. 2, p. 177.
9. Akselrud, L.G., Gryn, Y.N., and Zavalij, P.Yu, Abstracts of Papers, *12th Europ. Crystallogr. Meet*., 1985, p. 55.